

# Adenine derived inhibitors of the molecular chaperone HSP90—SAR explained through multiple X-ray structures

Brian Dymock,\* Xavier Barril, Mandy Beswick, Adam Collier, Nicholas Davies, Martin Drysdale, Alexandra Fink, Christophe Fromont, Roderick E. Hubbard, Andrew Massey, Allan Surgenor and Lisa Wright

*RiboTargets Ltd, Granta Park, Cambridge, CB1 6GB, UK*

Received 2 September 2003; revised 28 October 2003; accepted 7 November 2003

**Abstract**—Multiple co-crystal structures of an adenine-based series of inhibitors bound to the molecular chaperone Hsp90 have been determined. These structures explain the observed SAR for previously described compounds and new compounds, which possess up to 8-fold improved potency against the isolated enzyme. Anti-tumour cell potency and mechanism of action data is also described for the most potent compounds. These data should enable the design of more potent Hsp90 inhibitors.

© 2003 Elsevier Ltd. All rights reserved.

## 1. Introduction

Hsp90 is an ATP-dependent chaperone protein essential for the maturation and activity of a varied group of proteins involved in signal transduction, cell cycle regulation and apoptosis.<sup>1,2</sup> The ATPase activity can be inhibited with some selectivity by natural product antibiotics such as geldanamycin or radicicol (Fig. 1).<sup>3</sup> Recent studies with geldanamycin derivatives suggest that cancer cells are particularly sensitive to HSP90 inhibition.<sup>4</sup> Further in vivo and clinical data supports the hypothesis that the HSP90 family may be an appropriate target for anti-cancer drug development.<sup>5–10</sup>

Structures of the N-terminal domain (Nt-) of human HSP90 $\alpha$  have been published both as unliganded protein and in complex with a variety of inhibitors.<sup>11</sup> A seven-stranded beta sheet forms the backbone of the protein and four alpha helices are arranged such that they form a compact cavity in which resides the ATP binding site.

Recently, Chiosis et al. described the design of a series of purine analogues and measured binding affinity and cellular activity.<sup>12</sup> Here, we report the structure of Nt-HSP90 $\alpha$  complexed to inhibitor **1** (PU3) and the design

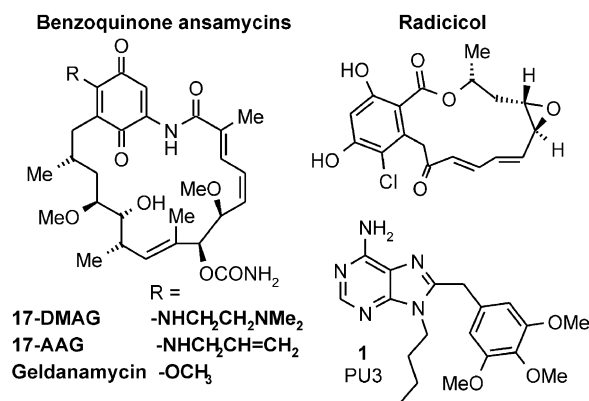


Figure 1. Structures of published Hsp90 inhibitors.

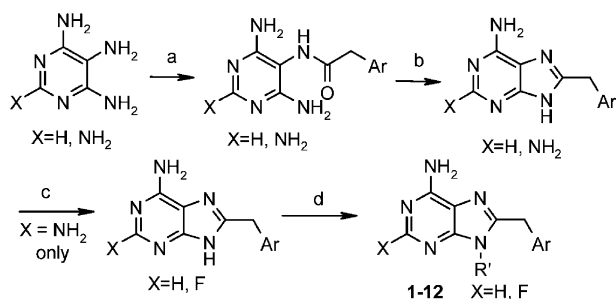
and structure determination of a series of analogues with enhanced enzyme inhibition. Detailed explanations of the observed changes in activity of these and other reported analogues of **1**<sup>13–15</sup> are now possible.

## 2. Synthesis

Scheme 1 depicts the preparation of compounds **1–12** starting from either 4,5,6-triaminopyrimidine, for 2-position hydrogen, or 2,4,5,6-tetraaminopyrimidine, for 2-position fluoro. This route is similar to the published synthesis of analogues of **1**<sup>13,16</sup> but with modifications to some reaction conditions. The first acylation proceeded

**Keywords:** HSP90; Chaperone; Adenine inhibitors; HSP70; Raf-1.

\* Corresponding author. Fax: +44-1223-895556; e-mail: [b.dymock@ribotargets.com](mailto:b.dymock@ribotargets.com)



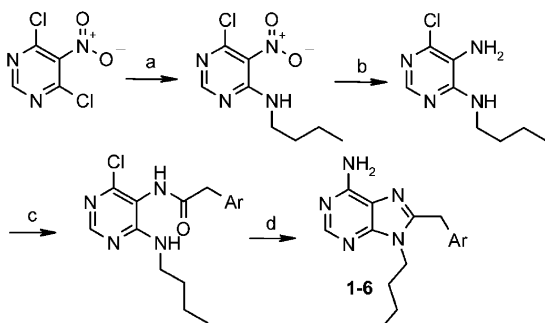
**Scheme 1.** Synthesis of purines from tri- or tetra-aminopyrimidine. Reagents and conditions: (a)  $\text{ArCH}_2\text{CO}_2\text{H}$ ,  $\text{Pr}_2\text{NEt}$ , HBTU, DMF, rt, 18 h; (b) thermal: NaOMe (15 equiv), EtOH, reflux, O/N; microwave: NaOMe (15 equiv), MeOH,  $\mu\text{wave}$ ,  $130^\circ\text{C}$ , 30 min; (c) HF-pyr (10 equiv), pyr,  $0^\circ\text{C}$ , 5 min then  $\text{tBuONO}$  (1.5 equiv),  $-20^\circ\text{C}$  to rt, 18 h; (d)  $\text{R}'\text{X}$ , NaOMe, DMF,  $0^\circ\text{C}$ , 5 min then to rt, 2 h.

most efficiently under HBTU conditions in DMF. Ring closure could either be performed thermally with excess methoxide or with a microwave reactor. HF in pyridine installs the 2-fluoro substituent with no protection of the purine required. The final alkylation step proved sluggish and low yielding with the published Mitsunobu conditions<sup>16</sup> so we developed alternative alkylation conditions, which gave good yields.<sup>17</sup>

Scheme 1 requires the alkyl group to be installed in a rather unsatisfactory final step and since the benzyl group was of greater importance to us, we developed a route, which not only installs the alkyl chain early in the synthesis but also improves overall reaction yields. Scheme 2 depicts this alternative synthesis starting from 4,6-dichloro-5-nitropyrimidine. Butylamine displacement installs the butyl chain efficiently followed by borohydride/nickel chloride reduction of the nitro group and acylation and cyclization of the resulting amine. Treatment with ammonia in the microwave gave the target compound.

### 3. Medicinal chemistry

In a malachite green ATPase assay<sup>18</sup> the  $\text{IC}_{50}$  of **1** was measured at  $>200 \mu\text{M}$  (Table 1). This is consistent with **1** being 20-fold less active than 17AAG ( $\text{IC}_{50} = 13.4$



**Scheme 2.** Synthesis of purines from 2,6-dichloro-5-nitropyrimidine. Reagents and conditions: (a)  $\text{tBuNH}_2$  (0.9 equiv)  $\text{Pr}_2\text{NEt}$  (0.9 equiv), THF, rt, 72 h; (b)  $\text{NaBH}_4$  (1.5 equiv),  $\text{NiCl}_2 \cdot 6\text{H}_2\text{O}$  (2 equiv), MeOH, rt, 1 h; (c)  $\text{ArCH}_2\text{CO}_2\text{H}$  (4 equiv),  $\text{Pr}_2\text{NEt}$  (11 equiv), MeCN, rt 18 h; (d) excess  $0.88 \text{NH}_3$ ,  $\mu\text{wave}$ ,  $130^\circ\text{C}$ , 30 min.

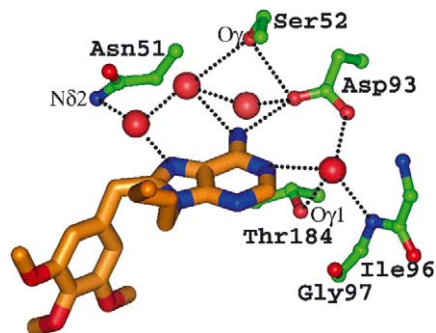
$\mu\text{M}$ ).<sup>12</sup> Despite its weak inhibition we were able to obtain a crystal structure of **1** bound to Hsp90.

Interaction with the key conserved Aspartic acid (Asp93) and a network of waters at the bottom of the ATP-binding pocket is seen in the crystal structures of the natural product inhibitors bound to Hsp90: the primary carbamate of geldanamycin and one of the hydroxyls of radicicol donate hydrogen bonds to Asp93 and other parts of the inhibitor structures accept hydrogen bonds from at least three of the four waters.<sup>3</sup> Like ADP, **1** donates an H-bond to Asp93 through its primary amine and interacts with the four waters as described above (Fig. 2). These interactions can be viewed as the critical ‘warhead’ component of the binding mode since any changes to these inhibitor groups abolish activity.

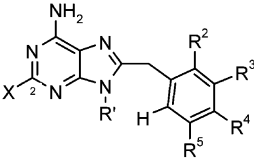
When **1** binds Hsp90 a conformational change of the backbone residues 104–111 occurs with the consequent creation of a new pocket in which the phenyl ring of **1** is bound. This lipophilic pocket is composed of Phe138, Met98, Val150, Leu103, Leu107, Trp162 and Tyr139, which remain in exactly the same conformation with respect to the ADP-Hsp90 structure. The aromatic ring of **1** is stacked between the side chains of Phe138 and Leu107, and forms other favourable hydrophobic interactions with Met98. Moreover, the methyls of the methoxy groups make favourable hydrophobic contacts with the aromatic rings of Trp162 and Tyr139, as well as with the aliphatic carbons of Ala111, Leu103 and Val150 (Fig. 3). Such close hydrophobic interactions lead to dramatic structure–activity relationships.

The length and nature of the methylene linker between the two ring systems is very important to provide **1** with the appropriate shape and size to occupy both the adenine binding site (Bergerat fold) and the new pocket. Larger linkers, such as  $(\text{CH}_2)_2$ , result in a misplacement of the phenyl ring, while conjugating groups, such as nitrogen, drive the rings towards a more co-planar orientation.

A single *meta*-methoxy benzyl group confers significantly better inhibitory activity than the trimethoxy benzyl in **1** (**3**,  $\text{IC}_{50} = 75 \mu\text{M}$ ) due to this methoxy group being buried in a very hydrophobic cavity, aligned by Met98 and Val150. Intriguingly, the single *para*-methoxy benzyl group (**2**) does not inhibit enzyme activity at

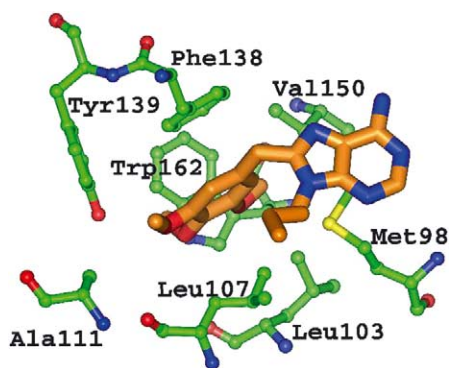


**Figure 2.** Key hydrogen bonds between **1**, Asp93 and water network.

**Table 1.** Purine analogues and enzyme inhibition data


Compd	X	R <sup>2</sup>	R <sup>3</sup>	R <sup>4</sup>	R <sup>5</sup>	R <sup>6</sup>	IC <sub>50</sub> ATPase (μM) <sup>a</sup>
AAG							13.4
Rd							<0.2
<b>1</b>	H	H	OMe	OMe	OMe	<i>n</i> -Butyl	>200
<b>2</b>	H	H	H	OMe	H	<i>n</i> -Butyl	>200
<b>3</b>	H	H	OMe	H	H	<i>n</i> -Butyl	75
<b>4</b>	H	H	OCH <sub>2</sub> O bridge	H	H	<i>n</i> -Butyl	15.3
<b>5</b>	H	OMe	H	H	OMe	<i>n</i> -Butyl	41
<b>6</b>	H	Cl	OMe	OMe	OMe	<i>n</i> -Butyl	>200
<b>7</b>	H	Cl	OMe	OMe	OMe	Pent-4-ynyl	>200
<b>8</b>	F	Cl	OMe	OMe	OMe	Pent-4-ynyl	30
<b>9</b>	F	OMe	H	H	OMe	H	53.5
<b>10</b>	F	OMe	H	H	OMe	<i>n</i> -Butyl	14.3
<b>11</b>	F	OMe	H	H	OMe	Pent-4-ynyl	4.1
<b>12</b>	F	H	OCH <sub>2</sub> O bridge	H	H	<i>n</i> -Butyl	17.1

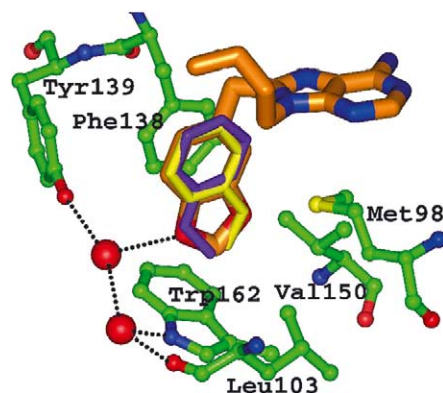
<sup>a</sup> All IC<sub>50</sub> values are the average of at least two determinations.

**Figure 3.** Interactions of **1** in lipophilic pocket.

200 μM. The presence of a void in the lipophilic pocket of the structure of **2**, results in poor packing between the ligand and its receptor.

Overlaying **3** with **2** led us to surmise that combination of both these features into a dioxolane five-membered ring would give an improved compound. Pleasingly, **4** had improved potency of around 5-fold over **3** (**4**, IC<sub>50</sub> = 15.3 μM). This compound exhibits the good features of **3** (good packing) and **2** (water mediated hydrogen bonds with Tyr139, Trp162 and Leu103) (Fig. 4).

Alternatively, installing an additional methoxy group in the *ortho*-position of **3** led to **5** with a small improvement in potency. The crystallographic structure of the complex reveals a water-mediated hydrogen bond of the oxygen of the *ortho*-methoxy with the nitrogen of Phe138, which could explain the increased activity. *ortho*-Chloro and bromo substitutions of the benzyl group in **1** have been studied by Chiosis et al.<sup>14</sup> Chloro has been reported to improve activity (compare **1** with **7**) whereas the larger bromo is approximately as active as hydrogen.<sup>14</sup> These activity differences are only seen in a binding

**Figure 4.** Overlay of the phenyl rings of **2** (purple) and **3** (yellow) with compound **4**. The carbon atoms are displayed in green (protein) and orange (ligand).

assay and not in the more stringent functional ATPase assay (**6** and **7** are >200 μM in the ATPase assay). The crystal structure of **7**-Hsp90 shows that the chlorine atom fits snugly making several hydrophobic contacts, particularly with Met98 and Phe138.

The scope for substitution at C2 is very limited due to the steric hindrance imposed by the backbone of Gly97. Given the almost perfect fit of the adenine ring into its cavity, it is unlikely that a bulky group would be tolerated in this position.

In our assay and as previously reported<sup>13</sup> fluoro substitution at C2 results in improved potency. However, we have observed a non-additive behaviour, ranging from more than 7× for the less active compounds (compare **7** and **8**) to less than 2× in favour of the butyl for the more active examples **12** and **4**. While **4** is more active than **5**, the equivalent 2-fluoro-adenine compounds (**12** and **10**) show very similar activities. In any case, the analysis of the crystallographic structures suggests that the purine ring and benzyl moieties add binding free energy by different mechanisms, which may or may not be complementary with specific combinations.

Preference for linear and flexible substituents on N9 of the purine<sup>14,15</sup> ring may be explained by the presence of Leu107 impeding the path out towards solvent (Fig. 3). The first few methylenes of the alkyl chain interact with residues Leu107 and Met98, while the rest of the side chain is completely solvent exposed explaining the relatively flat SAR observed in this area.

Within the more active 2,5-dimethoxy fluoro benzyl series (compounds **9–11**) the contribution of the 9-alkyl group can be more clearly demonstrated. With no substitution the potency is quite weak but still measurable at 53.5 μM (**9**). This compares favourably with the non-fluoro series where 9-H compounds were not active even at concentrations of 200 μM. When the butyl chain is installed (**10**), the potency improves by around 4-fold and by more than 14-fold with the pent-4-ynyl substituent (**11**). This may be due to an increased interaction between the acetylene group and the hydrophobic lip of the pocket.

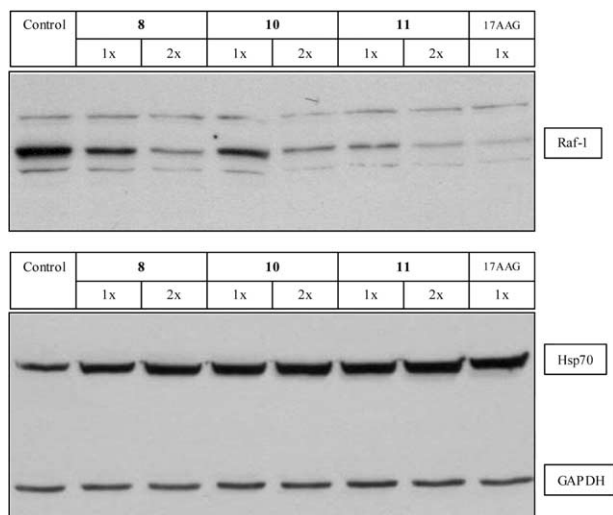


**Figure 5.** Western blots analysis showing an increase in Hsp70 and a decrease in c-Raf following exposure of HCT116 cells to 1- and 2-fold  $GI_{50}$  concentrations of compounds **8**, **10**, **11** and **17AAG** (control).

#### 4. Biology

The cellular activity of three of the most active ATPase inhibitors was measured using a Sulforhodamine B (SRB) growth inhibition assay on the human colon tumour cell line, HCT116. All three compounds (**8**, **10**, **11**) exhibited similar  $GI_{50}$  values (3.9, 3.4 and 3.3  $\mu$ M, respectively). This compares well with the  $GI_{50}$  described by Chiosis et al. for **8** in MCF-7 cells.<sup>14</sup> In order to distinguish between generalised and HSP90 inhibitor-specific cell growth inhibition, the upregulation of the co-chaperone HSP70 and down-regulation of the HSP90 client protein Raf-1 was measured at the cell growth inhibition  $GI_{50}$  value. It has been shown previously that this change in protein expression profile is due to specific HSP90 inhibition.<sup>18,19</sup> When exposed to these compounds the HCT116 cells demonstrated an increase in the levels of HSP70 and decrease in the levels of Raf-1 (Fig. 5).<sup>11</sup> This indicates that cell growth inhibition is occurring by a mechanism dependent on HSP90 inhibition.

#### 5. Conclusion

Structure–activity relationships for a series of purine inhibitors of the Hsp90 chaperone have been explained by multiple X-ray structures of the ligands bound to the target. Elucidation of the key hydrogen bonds and hydrophobic interactions should enable more potent inhibitors to be developed.

#### Acknowledgements

The authors are indebted to Joanne Wayne and Kate Grant for enzyme assays and Adam Hold and Heather Simmonite for analytical support.

#### References and notes

- Pearl, L. H.; Prodromou, C. *Curr. Opin. Struc. Biol.* **2000**, *10*, 46.
- Young, J. C.; Moarefi, I.; Hartl, F. U. *J. Cell. Biol.* **2001**, *154*, 267.
- Roe, S. M.; Prodromou, C.; O'Brien, R.; Ladbury, J. E.; Piper, P. W.; Pearl, L. H. *J. Med. Chem.* **1999**, *42*, 260.
- Chiosis, C.; Huezo, H.; Rosen, N.; Mimnaugh, E.; Whitesell, L.; Neckers, L. *Mol. Cancer Ther.* **2003**, *2*, 123.
- Egorin, M. J.; Zuhowski, E. G.; Rosen, D. M.; Sentz, D. L.; Covey, J. M.; Eiseman, J. L. *Cancer Chemother. Pharmacol.* **2001**, *47*, 291.
- Egorin, M.; Lagattuta, T.; Hamburger, D.; Covey, J.; White, K.; Musser, S.; Eiseman, J. *Cancer Chemother. Pharmacol.* **2002**, *49*, 7.
- Soga, S.; Sharma, S.; Shiotsu, Y. S.; Makiko, T.; Harunobu, Y.; Kazuo, I.; Yoji, M.; Chikara, T.; Tatsuya, K.; Junichi, S.; Theodor, W.; Neckers, L. M.; Akinaga, S. *Cancer Chemother. Pharmacol.* **2001**, *48*, 435.
- Banerji, U. O. D. A.; Scurr, M.; Benson, C.; Hanwell, J.; Clark, S.; Raynaud, F.; Turner, A.; Walton, M.; Workman, P.; Judson, I. *Proc. Am. Soc. Clin. Oncol.* **2001**, *20*, 82a.
- Munster, P. T. L.; Schwartz, L.; Larson, S.; Kenneson, K.; De La Cruz, A.; Rosen, N.; Scher, H. *Proc. Am. Soc. Clin. Oncol.* **2001**, *20*, 83a.
- Wilson, R. H.; Takimoto, C. H.; Adnew, E. B.; Morrison, G.; Grollman, F.; Thomas, R. R.; Saif, M. W.; Hopkins, J.; Allegra, C.; Grochow, L.; Szabo, E.; Hamilton, J. M.; Monahan, B. P.; Neckers, L. G.; Rem, J. L. *Proc. Am. Soc. Clin. Oncol.* **2001**, *20*, 82a.
- Jez, J.; Chen, J.-H.; Rastelli, G.; Stroud, R.; Santi, D. *Chem. Biol.* **2003**, *10*, 361.
- Chiosis, G.; Timaul, M. N.; Lucas, B.; Munster, P. N.; Zheng, F. F.; Sepp-Lorenzino, L.; Rosen, N. *Chem. Biol.* **2001**, *8*, 289.
- Chiosis, G. and Rosen, N. PCT WO 02/36075, 2002; *Chem. Abstr.* **2002**, *136*, 374828.
- Chiosis, G.; Lucas, B.; Shtil, A.; Huezo, H.; Rosen, N. *Bioorg. Med. Chem.* **2002**, *10*, 3555.
- Kasibhatla, S. R.; Hong, K.; Zhang, L.; Biamonte, M. A.; Boehm, M. F.; Shi, J.; Fan, J. PCT WO 03/037860, 2003; *Chem. Abstr.* **2003**, 356414.
- Lucas, B.; Rosen, N.; Chiosis, G. *J. Comb. Chem.* **2001**, *3*, 518.
- Data for **12**: Purified by flash chromatography eluting with  $CH_2Cl_2$ –2% MeOH/ $CH_2Cl_2$ .  $^1H$  NMR ( $CDCl_3$ , 7.26)  $\delta$  0.98 (t, 3H,  $J=7.5$  Hz), 1.39 (m, 2H), 1.68 (m, 2H), 4.05 (t, 2H,  $J=7.5$  Hz), 4.23 (s, 2H), 5.99 (s, 2H), 6.04 (s, 2H), 6.76 (dd, 1H,  $J=1.5, 8.0$  Hz), 6.80 (d, 1H,  $J=1.5$  Hz), 6.86 (d, 1H,  $J=8.0$  Hz). LC–MS retention time=2.31 min,  $m/z$  (EI): 344 ( $M^++1$ ). Anal. calcd for  $C_{17}H_{18}FN_5O_2$ : C, 59.41; H, 5.24; N, 20.39. Found: C, 59.57; H, 5.34; N, 20.01.
- Aherne, G.; Maloney, A.; Prodromou, C.; Rowlands, M.; Hardcastle, A.; Boxall, K.; Clarke, P.; Walton, M.; Pearl, L.; Workman, P. Assays for HSP90 and Inhibitors. In *Methods in Molecular Medicine: Novel Anticancer Drug Protocols*; Adjei, A., Buolamwini, J., Eds.; Humana: NJ, 2003; p 149.
- Workman, P. *Mol. Cancer Ther.* **2003**, *2*, 131.